



Molecular Crystals and Liquid Crystals

Publication details, including instructions for authors and subscription information:

<http://www.tandfonline.com/loi/gmcl16>

Lyotropic Liquid Crystals in Stagnation Flow: Fibrinogen

S. F. Emory^{a b} & A. A. Kozinski^{a c}

^a Department of Chemical Engineering, University of Illinois

^b The Dow Chemical Company, Pittsburg, California, 94565

^c The Quaker Oats Company, Barrington, Illinois, 60010

Version of record first published: 29 Aug 2007.

To cite this article: S. F. Emory & A. A. Kozinski (1975): Lyotropic Liquid Crystals in Stagnation Flow: Fibrinogen, Molecular Crystals and Liquid Crystals, 31:3-4, 305-318

To link to this article: <http://dx.doi.org/10.1080/15421407508082883>

PLEASE SCROLL DOWN FOR ARTICLE

Full terms and conditions of use: <http://www.tandfonline.com/page/terms-and-conditions>

This article may be used for research, teaching, and private study purposes. Any substantial or systematic reproduction, redistribution, reselling, loan, sub-licensing, systematic supply, or distribution in any form to anyone is expressly forbidden.

The publisher does not give any warranty express or implied or make any representation that the contents will be complete or accurate or up to date. The accuracy of any instructions, formulae, and drug doses should be independently verified with primary sources. The publisher shall not be liable for any loss, actions, claims, proceedings, demand, or costs or damages whatsoever or howsoever caused arising directly or indirectly in connection with or arising out of the use of this material.

Lyotropic Liquid Crystals in Stagnation Flow: Fibrinogen

S. F. EMORY† and A. A. KOZINSKI‡

Department of Chemical Engineering, University of Illinois

(Received March 24, 1975; in final form July 14, 1975)

A lyotropic liquid crystal, a concentrated fibrinogen solution, was formed in a two-dimensional axial stagnation flow field. The stagnation surface was a water permeable but fibrinogen impermeable membrane. The rejection of fibrinogen at the stagnation surface causes the concentration at the surface to exceed the value for mesophase formation. Optical techniques were used to detect the existence of a liquid crystal at the membrane surface. Pressure measurements agreed with theoretical models. For many applications the theoretical models reduce to an effective Newtonian description.

INTRODUCTION

The anisotropic behavior of thermotropic liquid crystals has been the focus of much recent research. In contrast, the lyotropic liquid crystal has been the subject of only a few recent studies. This is undoubtedly due to a scarcity of suitable systems and the lack of real applications. However, the role of lyotropic liquid crystals in living systems appears to be of critical importance.

A better understanding of the role of liquid crystals in living systems could be attained if valid simple descriptions of their dynamic behavior were available. The following in-vitro studies with the protein fibrinogen were made to evaluate the formation and dynamic behavior of a lyotropic liquid crystal system. The controlling hydrodynamic equations in two-dimensional axial flow will be solved and the results will be compared to experimental data.

† S. F. Emory is now with The Dow Chemical Company, Pittsburg, California, 94565.

‡ A. A. Kozinski is now with The Quaker Oats Company, Barrington, Illinois, 60010.

ANALYTICAL DESCRIPTION

The particular situation we are treating is that of a thin region of liquid crystal which forms a boundary to a much larger isotropic region. Both regions are in a continuous momentum field. This is illustrated in Figure 1 for axially symmetric stagnation flow. This flow geometry consists of flow along an axis perpendicular to a porous surface. The presence of the partially permeable surface forces the flow to divide; part of which goes through the surface while the other portion is forced to flow parallel to the surface. As macromolecules are brought to the surface by convection, they will be rejected while water will pass through. This will cause the concentration in the vicinity of the surface to increase to the level where a mesophase forms. For this situation, the linearized continuum mechanics of Aslaksen¹ are particularly useful. Although his description creates the awkward director vector to denote molecular orientation, the formulation still proves to be useful in simplified form.

The conservation of linear momentum is as follows:

$$\rho v_j \frac{\partial v_i}{\partial x_j} = - \frac{\partial P}{\partial x_i} + \text{Div}(\sigma)$$

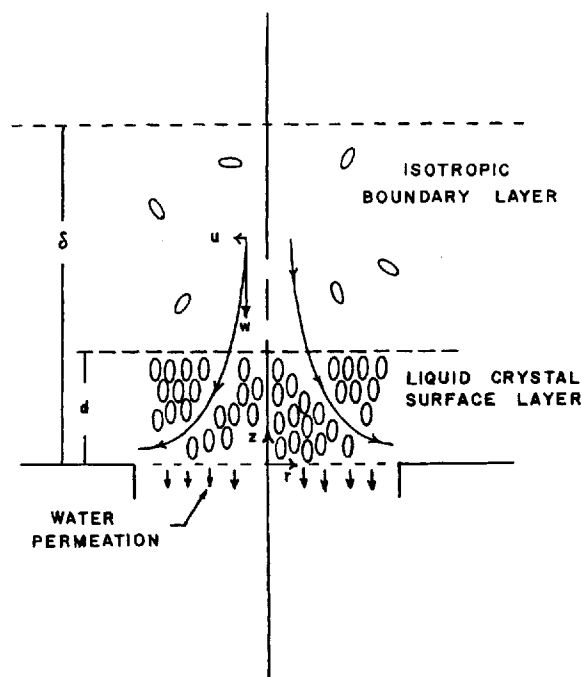


FIGURE 1 Proposed two phase stagnation flow model.

The specific application of this relation requires a constitutive relation which fits the particular symmetries of the liquid crystal being studied. The relations of Aslaksen are for a nematic crystal.

$$\sigma_{ij} = \alpha_1 L_k L_p A_{kp} L_i L_j + \alpha_2 L_i N_j + \alpha_3 L_j N_i + \alpha_4 A_{ij} \\ + \alpha_5 L_i L_k A_{kj} + \alpha_6 L_j L_k A_{ki}$$

The coefficients α_i have the dimensions of a viscosity. The vector L is defined as a unit vector representing the molecular orientation. The tensor A is the symmetric portion of the velocity gradient; the antisymmetric part is ω . The vector N represents the rate of change of L with respect to the surrounding fluid. The individual components are

$$A_{ij} = \frac{1}{2} \left(\frac{\partial v_i}{\partial x_j} + \frac{\partial v_j}{\partial x_i} \right) \\ \omega_{ij} = \frac{1}{2} \left(\frac{\partial v_i}{\partial x_j} - \frac{\partial v_j}{\partial x_i} \right) \\ N_i = \frac{\partial L_i}{\partial t} + v_j \frac{\partial L_i}{\partial x_j} + \omega_{ki} L_k$$

In general the solution of these equations is very complex. However, simple results can be obtained for very thin layers near a phase boundary.

The usual Prandtl boundary layer concepts reduce this description to a pseudo Newtonian approximation. This is summarized in the Appendix. In this study the description will be applied to stagnation flow which as with boundary layer flows leads to useful simple solutions. For orientation of the liquid crystal perpendicular to the stagnation surface the director is then defined:

$$L = (\sin \theta, \cos \theta) = (0, 1)$$

where θ is the angle between the aligned molecules and the axial velocity W . We can further assume that at steady state L does not vary with position, and N reduces to:

$$N_i = \omega_{ki} L_k$$

For axial-symmetric flow the following simplifying transformations are made:

$$\omega = -2f(z), \quad u = rf'(z)$$

$$P_0 - P = \frac{\delta}{2} a^2 (r^2 + f(z))$$

The applicable boundary conditions are:

$$z = 0, u = 0, \omega = V_p \\ z = \delta \quad u = U$$

The momentum equations reduce to

$$f'^2 - 2ff'' = a^2 + \frac{\alpha_4}{\rho r^2} f' + \frac{1}{\rho} \frac{1}{2} (-\alpha_2 + \alpha_4 + \alpha_5) f'''$$

$$2ff' = \frac{a^2}{4} f' - \frac{1}{\rho} ((\alpha_3 + \alpha_4 + \alpha_6) + 2(\alpha_1 + \alpha_5)) f''$$

In the above equations the terms α_4 , $(-\alpha_2 + \alpha_4 + \alpha_5)$, and $(\alpha_3 + \alpha_4 + \alpha_6)$ are recognized as twice the viscosities when the molecules slide past each other against their short sides, ends and long sides, respectively.

These results can be compared to the well known Newtonian results

$$f'^2 - 2ff'' = a^2 + \nu f'''$$

$$2ff' = \frac{a^2}{4} F - \nu f''$$

The constant a is a constant proportional to the frictionless velocity U . The anisotropic description can be reduced to the same form if α_1 , α_4 , α_5 can be neglected. These coefficients have been found to be small for some liquid crystals. No data are available for α_5 , but it will be neglected in this study. This reduces the model to a description which accounts for only the gross effects of structure and, thus, is not limited to a particular class of liquid-crystals. The asymmetric equations then have the same form as the Newtonian equations with end to end and long side viscosities being associated with the radial and axial components, respectively. A similar result can be obtained for the orientation parallel to the membrane surface in which θ has a value approaching 90° . The end to end and side to side viscosities are exchanged in the component momentum equations.

NUMERICAL SOLUTION

To solve the simplified description, the end to end and long side viscosities are required for the particular liquid crystal under study. Approximate values can be obtained from the work of Kozinski *et al.*,³ who measured the viscosity (as measured by a capillary tube viscometer) of concentrated fibrinogen solutions. Above a 20 weight percent solution a liquid crystal phase was found to exist. The results are reproduced here as Figure 2. The maximum at the transition to the liquid crystal is about 10^6 poise. If one assumes a Flory lattice model,⁴ this maximum value represents the dissipation due to random movement of highly compacted large particles. The major contribution should be that of end to end resistance. Thus, this maximum

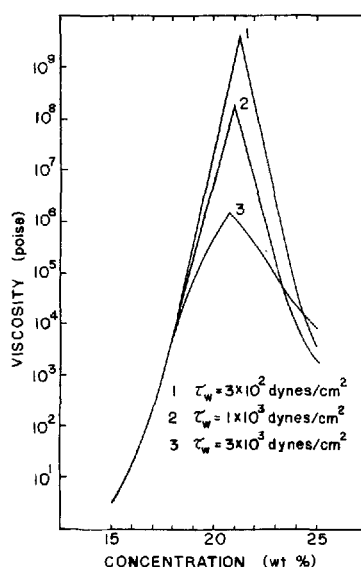


FIGURE 2 Viscosity of aqueous fibrinogen solutions from Kozinski *et al.*³

should indicate the order of magnitude of the end to end resistance. Similarly, the well developed liquid crystal viscosity should represent the long side viscosity—about 10 poise. The isotropic dilute solution will have a viscosity of about .01 poise.

Using the above viscosity values a numerical solution to the descriptive equations can be obtained through the use of Runge Kutta techniques. Two situations were compared. First the bulk layer and surface layer are treated as Newtonian fluids with a viscosity difference of 10^8 poise. Second the bulk remained Newtonian but the surface layer was treated as a liquid crystal with orientation perpendicular to the support surface.

In applying the numerical technique the thickness, d of the mesophase surface layer (Region 1 in Figure 1) will be determined by a mass balance:

$$C_2(-w)\Pi r^2 = \int_0^d u C_1 2\Pi r \, dz$$

where the concentrations, C_1 and C_2 , to a first approximation were assumed constant in their respective phases.

Pertinent results are shown in Table I. Notice the large predicted pressure drops for the Newtonian case. In contrast the liquid crystal model predicts only very small pressure drops. Figures 3 and 4 illustrate these results for the entire regions. The velocity profiles are identical for both cases since in the thin layer the same viscosity is used in the radial momentum equation

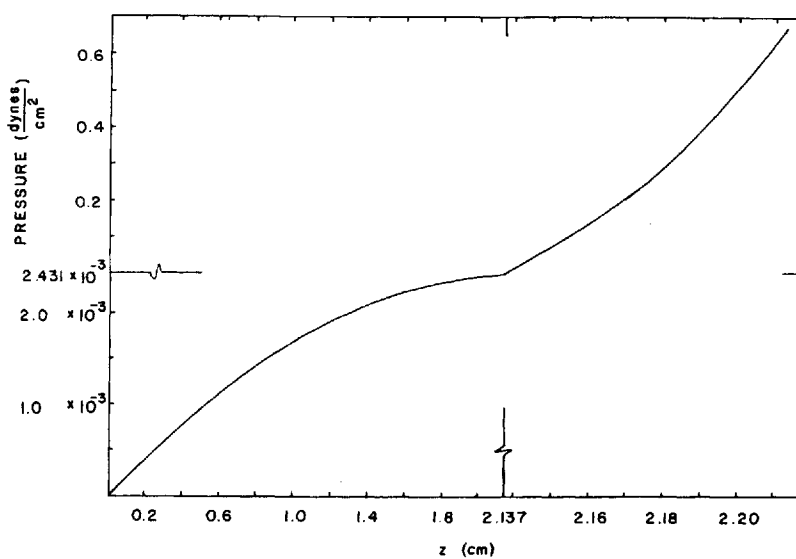


FIGURE 3 Calculated flow functions for the Newtonian analysis.

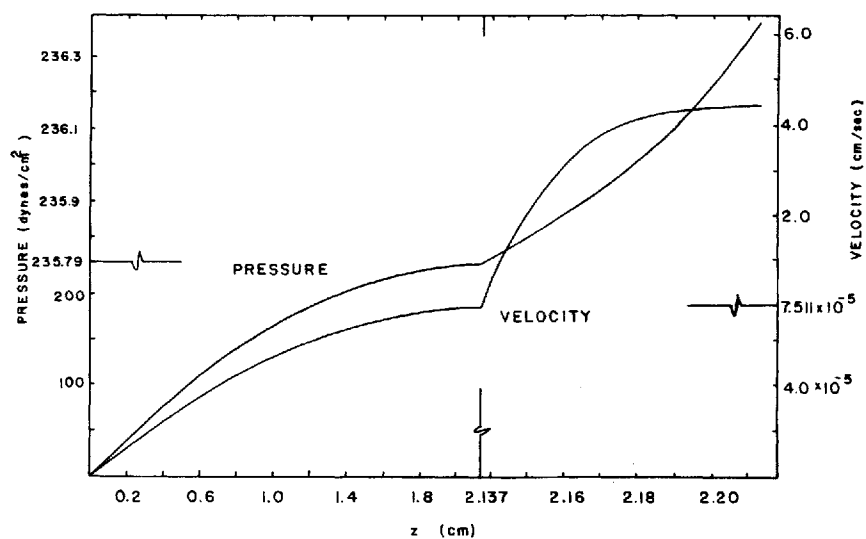


FIGURE 4 Calculated flow functions for the anisotropic analysis.

for both the Newtonian and liquid crystal cases. Thus the models predict the lack of a significant pressure drop when a liquid crystal layer is present and oriented perpendicular to the support surface.

EXPERIMENTAL

The experimental tests consisted of using a permeable stagnation flow cell to verify the possibility of creating a liquid crystal layer and, secondly, to determine the pressure drop across this layer. The lyotropic material used was aqueous solutions of bovine fibrinogen. Kozinski, *et al.*³ have determined that concentrated solutions of fibrinogen have the optical and viscosity characteristics of a nematic mesophase. However, the lack of definitive x-ray data prevent the absolute classification of this mesophase. The flow system shown in Figures 5 and 6 was constructed of stainless steel. At the stagnation

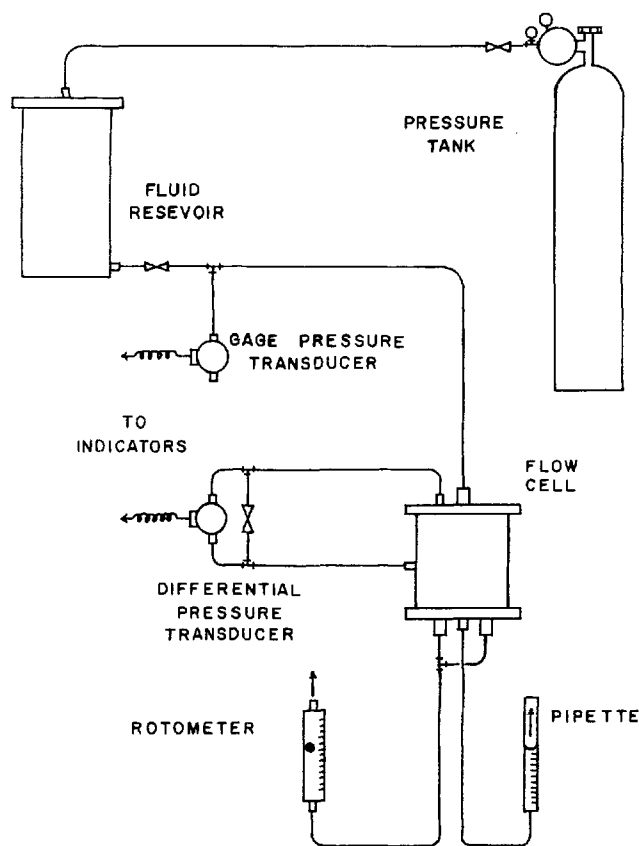


FIGURE 5 Experimental flow system.

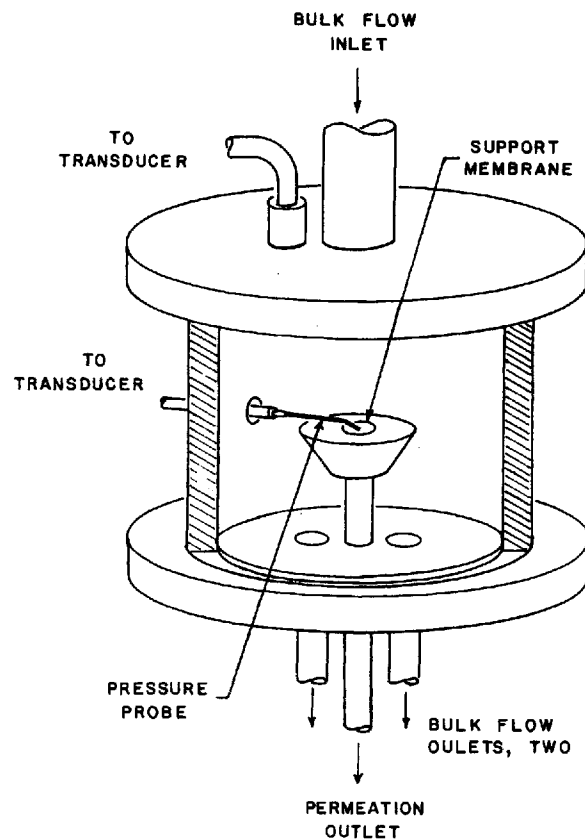


FIGURE 6 Permeable stagnation flow cell.

point was a porous stainless steel disc which supported a porous Millipore Pellicon PSED membrane. This membrane retained 100% of the fibrinogen while allowing water and other small ions to pass freely. With a dilute solution of fibrinogen introduced at the top of the cell, the conditions of two dimensional axial symmetric flow are met at the membrane surface. Water passes through the membrane while fibrinogen is rejected. This creates a highly concentrated layer of fibrinogen at the surface. By adjusting conditions, the surface concentration exceeded that necessary to form a liquid crystal phase. The phase thus formed at the membrane surface will be in a two-dimensional velocity field composed of the permeation velocity through the membrane and the cross velocity across the membrane.

The pressure measurements across the layer were made with a Pace differential transducer (C. J. Enterprises) model CJVR with a G212 indicator.

TABLE I
Brief results of the numerical solutions

	z (cm)	u (cm/sec)	w (cm/sec)	pressure (dynes/cm ²)	
				Newtonian	anisotropic
low flow ($Q = 90$ cc/sec)	0.0	0.0	0.2840	0.0	0.0
	$d = 4.258$	4.876×10^{-5}	0.2844	152.87	1.651×10^{-3}
	$\delta = 4.365$	1.786	0.7476	153.17	0.3123
medium flow ($Q = 223$ cc/sec)	0.0	0.0	0.2206	0.0	0.0
	$d = 2.137$	7.511×10^{-5}	0.2209	235.73	2.431×10^{-3}
	$\delta = 2.213$	4.425	1.052	236.40	0.6719
high flow ($Q = 3600$ cc/sec)	0.0	0.0	0.2497	0.0	0.0
	$d = 0.3480$	5.403×10^{-2}	0.2501	1648.0	1.657×10^{-2}
	$\delta = 0.3691$	71.44	3.895	1657.7	9.835
Newtonian v	0.0	0.0	0.2497		
is 10 poise,	$d = 4.237 \times 10^{-3}$	5.403×10^{-2}	0.2500		
high flow	$\delta = 2.524 \times 10^{-2}$	71.44	3.865		

The surface pressure was obtained using a probe of 25 gauge tubing which should give the pressure at a point a few microns above the membrane still within the liquid crystal layer. Pressures were recorded at 0.2 cm and 0.635 cm from the membrane center. The transducer/indicator equipment had a precision of 69 dynes/cm² (0.001 psi) and an accuracy of approximately twice the precision. The system was maintained at 10 ± 1 psig. The bulk flow which was monitored with a rotameter was varied for the different flow conditions. The permeation flow rate was measured by timing the flow through a micro-pipette. All data were obtained at the three bulk flow rates corresponding to the three conditions shown in Table I.

The apparatus used to obtain the separate optical data is shown in Figure 7. Light from a high intensity incandescent light source was conducted to the concentrated layer by means of a 10 mil DuPont crofon light guide. This light guide and a similar receiving guide were capped with crossed (90°) polaroid sheets. The light collected by the receiving guide was then conducted to the densitometer portion of a spectrophotometer. The retaining sleeves were made of 16 gauge tubing which positioned the center line of the light path 0.083 cm above the membrane surface. The existence of birefringence could be determined by rotating both polaroid caps. More experimental detail can be found in Emory.⁵

RESULTS

The existence of a structured layer is indicated by the results of the optical measurements shown in Figure 8. The actual molecular orientation, parallel

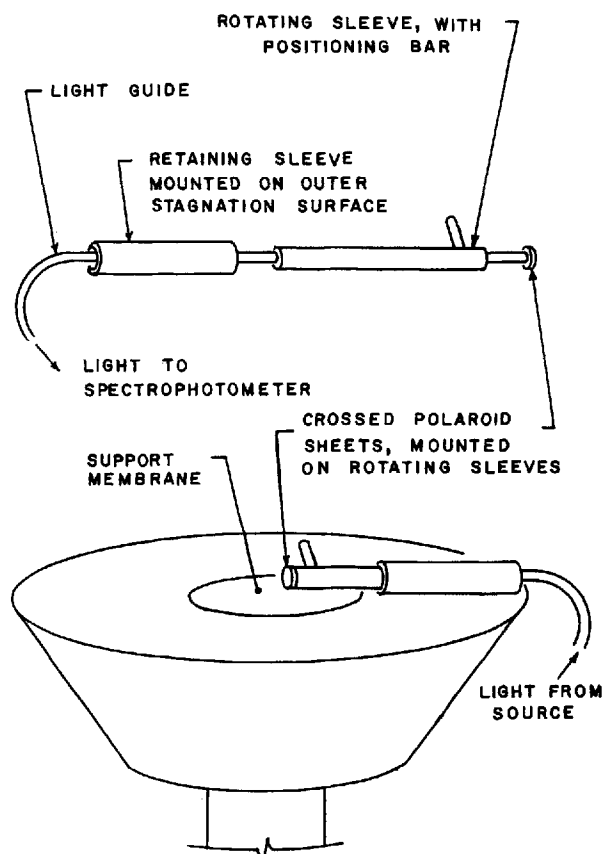


FIGURE 7 Schematic of optical system used on stagnation surface.

or perpendicular to the membrane surface, cannot be determined from these measurements. However, the previously summarized viscosity data and the hydrodynamic description of a liquid crystal suggest that the molecular orientation is perpendicular to the support surface. The pressure drop measurements also confirmed this interpretation. For all of the conditions of Table I the dynamic pressure drop across the concentrated layer was zero to within experimental accuracy. This agreed with our simplified anisotropic hydrodynamic description with molecular orientation perpendicular to the surface.

Overall the study indicated that a lyotropic mesophase of fibrinogen can be created in a two dimensional flow field. Control of the momentum field should permit in the future, control of the molecular orientation relative to the support surface.

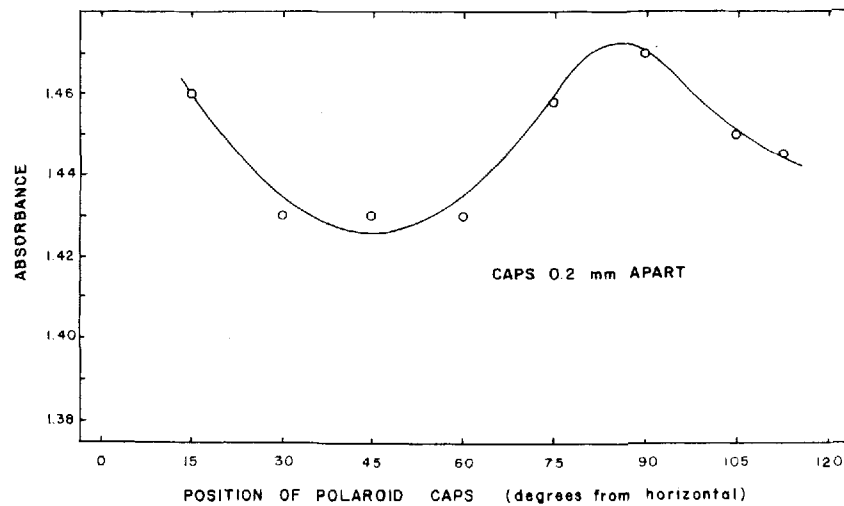


FIGURE 8 Birefringence measurements for the concentrated layer on the stagnation surface.

The observed zero pressure drop was contrary to the results normally predicted for ultrafiltration where large pressure drops are predicted to occur across the concentrated layer. Our results indicate that a zero pressure drop is the result of the formation of a liquid crystal phase and the resulting anisotropy. It is worthwhile to note that many of the substances commonly separated by ultrafiltration are large asymmetric molecules and therefore are potentially structured in concentrated layers. As such, control of orientation could possibly reduce the large pressure drops which occur in ultrafiltration. Likewise the use of ultrafiltration conditions make it possible to easily create lyotropic mesophases from a wide variety of asymmetric solutes.

The simplified hydrodynamic models should provide a useful framework for understanding liquid crystal layers in natural systems where thin layers are the most common situation.

Appendix: General boundary layer analysis

For a general two dimensional flow shown in Figure A1 with the director assumed to be restricted to the x, z plane and with θ , the angle with the z axis, the director has the following value:

$$L = (\sin \theta, 0, \cos \theta)$$

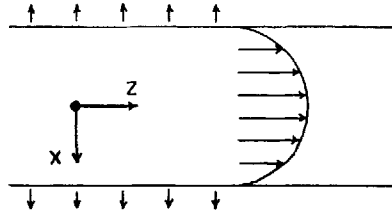


FIGURE A-1 Flow model for permeable channel flow.

The momentum equation for the z component in dimensionless form becomes

$$u^0 \frac{\partial u^0}{\partial z^0} + v^0 \frac{\partial u^0}{\partial x^0} = - \frac{\partial P^0}{\partial z^0} + \frac{1}{\text{Re } \eta_{\text{eff}}} \left[\frac{\partial \sigma_{zz}}{\partial z} + \frac{\partial \sigma_{xz}}{\partial x} \right]$$

$$\text{Re} = \frac{\rho U_{\infty} l}{\eta_{\text{eff}}}$$

If we now assume the usual boundary layer requirement that the thickness of the layer for momentum transport, δ , is much less than the characteristic length, l , then the usual simplifications can be made by neglecting all terms less than order $1/\delta$.

$$u^0 \frac{\partial u^0}{\partial z^0} + v^0 \frac{\partial u^0}{\partial x^0} = - \frac{\partial P^0}{\partial z^0} + \frac{1}{\text{Re}} \frac{\partial^2 u^0}{\partial x^{02}}$$

$$\eta_{\text{eff}} \equiv \frac{1}{2} (\alpha_3 + \alpha_4 + \alpha_6)$$

This definition of η_{eff} is just the value for the molecules sliding past each other in their long direction. Similarly for the x component equation

$$\frac{\partial P^0}{\partial x^0} = \frac{1}{\text{Re}} \frac{1}{\eta_{\text{eff}}} \frac{\partial}{\partial x^0} \left\{ \frac{1}{2} \theta (\alpha_2 + \alpha_3 + \alpha_5 + \alpha_6) \frac{\partial u^0}{\partial x^0} \right\}$$

For very small values of θ this reduces down to the usual boundary layer result that

$$\frac{\partial P^0}{\partial x^0} = 0$$

The other limit with $\theta \approx 90^\circ$ can similarly be developed.

$$U^0 \frac{\partial u^0}{\partial z^0} + V^0 \frac{\partial u^0}{\partial x^0} = - \frac{\partial P^0}{\partial z^0} + \frac{1}{\text{Re}} \frac{\partial^2 u^0}{\partial x^{02}}$$

$$\eta'_{\text{eff}} = \frac{1}{2} (-\alpha_2 + \alpha_4 + \alpha_5)$$

Thus the form of the z component of the momentum equation is the same as in the parallel orientation case except that the effective viscosity is now that for end to end resistance.

The x equation for angles very close to 90° reduces to the no pressure drop approximation of Newtonian flow. The first order correction for orientations only approaching 90° is as follows:

$$\frac{\partial P^0}{\partial x^0} = \frac{1}{\text{Re}} \frac{1}{\eta'_{\text{eff}}} \left[\frac{1}{2} (\alpha_1 + \alpha_2 + \alpha_3 + \alpha_5 + \alpha_6) \frac{\partial}{\partial x^0} \left(\frac{\Pi}{2} - \theta \right) \frac{\partial u^0}{\partial x^0} \right]$$

Thus within the limits of our model the liquid crystal layer may be treated as a Newtonian boundary layer with appropriate single direction viscosity in each component equation. This extends to more useful geometries the results developed in this paper for stagnation flow.

Symbols used in this article

Symbol	Meaning
A	Symmetric portion of the velocity gradient, sec^{-1} .
C	Concentration, moles · liter $^{-1}$.
D	Diameter, cm, in.
F	Transformed pressure function, cm^2 .
G	Function vector, used in numerical solution.
L	Director (represents orientation of molecules).
N	Rate of change of L with respect to surrounding fluid, sec^{-1} .
P	Correction vector, used in numerical solution.
Q	Bulk flow rate, $\text{cm}^3 \cdot \text{sec}^{-1}$.
U	Frictionless radial velocity, $\text{cm} \cdot \text{sec}^{-1}$.
V_p	Permeation velocity, $\text{cm} \cdot \text{sec}^{-1}$.
W	Frictionless axial velocity, $\text{cm} \cdot \text{sec}^{-1}$.
a	Cell constant, sec^{-1} .
d	Concentrated layer thickness, cm.
f	Transformed velocity function, $\text{cm} \cdot \text{sec}^{-1}$.
g	Component of G .
h	Step size of ξ (used in numerical integration), dimensionless.
P	Pressure, dynes · cm^{-2} .
P_0	Pressure at the stagnation point, dynes · cm^{-2} .
r	Radial coordinate, cm.
t	Time, sec.
u	Radial velocity, $\text{cm} \cdot \text{sec}^{-1}$.
v	General velocity, $\text{cm} \cdot \text{sec}^{-1}$.
w	Axial velocity, $\text{cm} \cdot \text{sec}^{-1}$.

x	General coordinate, cm.
z	Axial coordinate, cm.
α	Coefficient of viscosity, poise.
δ	Boundary layer thickness, cm.
ξ	Dimensionless axial coordinate variable.
ν	Kinematic viscosity, $\text{cm}^2 \cdot \text{sec}^{-1}$.
ρ	Density, $\text{g} \cdot \text{cm}^{-3}$.
σ	Shear (tensor), $\text{dynes} \cdot \text{cm}^{-2}$.
ϕ	Transformed velocity function, dimensionless.
ω	Antisymmetric portion of velocity gradient.

References

1. E. W. Aslaksen, *Phys. Kondens. Materie*, **14**, 80 (1971).
2. M. Miesowicz, *Nature*, **158**, 27 (1945).
3. A. A. Kozinski, G. J. Kizior, and S. G. Wax, *AIChE Journal*, **20**, 1104 (1974).
4. P. J. Flory, *Proc. Roy. Soc. (London)*, **A234**, 73 (1956).
5. S. F. Emory, "Stagnation Flow in a Liquid Crystal," M.S. Thesis, University of Illinois (1974).